Tl_2AXTe_4 (A = Cd, Hg, Mn; X = Ge, Sn): Crystal Structure, Electronic Structure, and Thermoelectric Properties

Michael A. McGuire,[†] Thomas J. Scheidemantel,[‡] John V. Badding,[§] and Francis J. DiSalvo*,[||]

Department of Physics, Clark Hall, Cornell University, Ithaca, New York 14853, Departments of Physics and Chemistry and Materials Research Institute, The Pennsylvania State University, University Park, Pennsylvania 16802, and Department of Chemistry and Chemical Biology, Baker Laboratory, Cornell University, Ithaca, New York 14853

Received August 11, 2005. Revised Manuscript Received September 21, 2005

The six new compounds $Tl_2CdGeTe_4$, $Tl_2CdSnTe_4$, $Tl_2HgGeTe_4$, $Tl_2HgSnTe_4$, $Tl_2MnGeTe_4$, and $Tl_2MnSnTe_4$ have been synthesized. All six compounds are isostructural and crystallize in the tetragonal space group *I*-42*m* with $a \approx 8.3$ Å and $c \approx 7.1$ Å. The structure is composed of chains of composition $[AXTe_4]^{2-}$ separated by Tl^{1+} ions, an ordered superstructure of the TlSe structure type. In addition to their syntheses and crystal structures, we report the calculated electronic structures of these six compounds and of the related compounds $KInTe_2$ and $TlInTe_2$. We measured the thermoelectric properties (electrical resistivity, thermopower, and thermal conductivity) of $Tl_2CdGeTe_4$, $Tl_2CdSnTe_4$, $Tl_2HgGeTe_4$, and $Tl_2HgSnTe_4$. These compounds are semiconductors with very low thermal conductivities and moderately high thermopowers. However, as currently prepared they have resistivities that are too high for thermoelectric applications. Magnetic susceptibility and resistivity measurements show $Tl_2MnGeTe_4$ and $Tl_2MnSnTe_4$ to be Mott insulators, in agreement with spin-polarized band structure calculations.

Introduction

In thermoelectric (TE) materials the coupling between entropy currents and particle currents allows for the direct conversion between thermal and electrical energy.[1] This makes possible the construction of refrigerators and electrical power generators with no moving parts which are compact and reliable. However, present devices operate with low efficiencies, and better materials are needed to improve their performance. The best-known TE materials for cooling applications near room temperature are doped, small band-gap semiconductors composed of heavy elements. The low Debye temperatures in these compounds, due to the presence of heavy atoms, lead to low lattice thermal conductivities. This is advantageous since the maximum efficiency of a TE material operating at absolute temperature *T* depends on the dimensionless figure of merit *ZT* defined by $ZT = S^2T/\rho\kappa$.[1] Here *S* is the Seebeck coefficient or thermopower, ρ is the electrical resistivity, and κ is the thermal conductivity. The highest *ZT* at room temperature is realized in doped alloys of Bi_2Te_3, Sb_2Te_3, and Sb_2Se_3 which have $|S| \approx 220$ μV/K, $\rho \approx 1$ mΩ cm, and $\kappa \approx 15$ mW/cm K, giving $ZT \approx 1$.[2] If $ZT = 4$ could be achieved, then the TE efficiency would equal that of residential compressor-based refrigerators.[3] This could open the way to widespread applications for TE coolers. It is unlikely that large increases in *ZT* will be realized through modifications of currently known materials. Significant improvement in TE performance in bulk materials will likely occur only through the discovery of new compounds with enhanced TE properties.

One active area of TE materials research is the synthesis and characterization of new alkali-metal chalcogenides. In particular, $CsBi_4Te_6$ has been shown to outperform Bi_2Te_3-based alloys below room temperature.[4] We have recently begun investigating Tl-containing compounds as TE materials.[5] Tl prefers the +1 oxidation state, and its chemistry is similar to that of the alkali metals. However, Tl is less electropositive than any alkali metal, which could lead to lower electrical resistivities and smaller band gaps. Tl is also heavier than any stable alkali metal and thus should form compounds with lower thermal conductivities. Indeed, we have shown in our recent study of multinary Tl chalcogenides that Tl-containing materials have measured band gaps consistently smaller than their isostructural alkali-metal analogues.[5] These compounds were also seen to have extremely low thermal conductivities. Some ternary Tl compounds have already been found to have interesting TE properties, including Tl_9BiTe_6,[6] Tl_2SnTe_5,[7] and $TlSbTe_2$.[8] The solid solution $TlIn_{1-x}Yb_xTe_2$, similar in structure to the

* To whom correspondence should be addressed. E-mail: fjd3@cornell.edu.
† Department of Physics, Cornell University.
‡ Department of Physics and Chemistry and Materials Research Institute, The Pennsylvania State University.
§ Department of Chemistry, The Pennsylvania State University.
|| Department of Chemistry and Chemical Biology, Cornell University.

(1) Heikes, R. R.; Ure, R. W., Jr. *Thermoelectricity: Science and Engineering*; Interscience Publishers: New York, London, 1961.
(2) Yim, W. M.; Rosi, F. D. *Solid-State Electron.* **1972**, *15*, 1121.
(3) DiSalvo, F. J. *Science* **1999**, *285*, 703.
(4) Chung, D.-Y.; Hogan, T.; Brazis, P.; Rocci-Lane, M.; Kannewurf, C.; Bastea, M.; Uher, C.; Kanatzidis, M. G. *Science* **2000**, *287*, 1024.
(5) McGuire, M. A.; Reynolds, T. K.; DiSalvo, F. J. *Chem. Mater.* **2005**, *17*, 2875.
(6) Wölfing, B.; Kloc, C.; Teubner, J.; Bucher, E. *Phys Rev. Lett.* **2001**, *86*, 4350.
(7) Sharp, J. W.; Sales, B. C.; Mandrus, D. G.; Chakoumakos, B. C. *Appl. Phys. Lett.* **1999**, *74*, 3794.

10.1021/cm0518067 CCC: $30.25 © 2005 American Chemical Society
Published on Web 10/27/2005

Table 1. Crystallographic Information for the Six Compounds Reported in This Work

Tl_2AXTe_4	$Tl_2CdGeTe_4$	$Tl_2CdSnTe_4$	$Tl_2HgGeTe_4$	$Tl_2HgSnTe_4$	$Tl_2MnGeTe_4$	$Tl_2MnSnTe_4$
a (Å)	8.3825(19)	8.4250(4)	8.3571(11)	8.397(4)	8.399(3)	8.4503(13)
c (Å)	7.0775(18)	7.2171(5)	7.0684(14)	7.157(6)	6.963(3)	7.1078(15)
V (Å^3)	497.3(2)	512.27(5)	493.67(13)	504.6(6)	491.2(3)	507.55(15)
size (μm^3)	100 × 50 × 30	200 × 70 × 10	100 × 100 × 40	100 × 70 × 40	150 × 30 × 30	50 × 30 × 20
θ range (deg)	3.44−30.41	3.42−30.44	3.45−28.56	3.43−30.45	3.43−30.41	3.41−30.46
reflns coll./unique	2921/404	5638/424	2372/345	2845/418	3478/405	3939/422
R_{int}	0.0442	0.0531	0.0894	0.0409	0.054	0.0603
completeness to θ max (%)	100	100	98.6	100	100	100
data/params	404/14	424/15	345/15	418/15	405/14	422/15
GOF on F^2	1.217	1.133	1.166	1.164	1.127	1.135
R1, $I > 2\sigma$	0.0234	0.0221	0.0488	0.0264	0.0255	0.0286
wR2, $I > 2\sigma$	0.0505	0.0480	0.1166	0.0544	0.0508	0.0580
R1, all data	0.0253	0.0224	0.0502	0.0277	0.0302	0.0368
wR2, all data	0.0509	0.0481	0.1172	0.0548	0.0524	0.0599
Flack param	0.019(15)	0.442(18)	0.27(3)	0.317(13)	0.064(19)	0.56(7)
largest difference peak and hole (e/Å^3)	1.311	1.627	4.893	1.181	1.640	0.989
	−2.176	−2.083	−3.118	−3.736	−3.056	−2.786
crystallographic coordinates for Te at position (x, x, z)						
x Te	0.1749(1)	0.1821(1)	0.1757(1)	0.1826(1)	0.1729(1)	0.1794(1)
z Te	−0.2252(1)	0.2396(1)	0.2254(2)	0.2406(1)	0.2316(1)	0.2468(2)
isotropic displacement parameters						
Tl	0.019(1)	0.021(1)	0.017(1)	0.018(1)	0.019(1)	0.021(1)
A	0.014(1)	0.013(1)	0.015(1)	0.013(1)	0.015(1)	0.013(1)
X	0.009(1)	0.010(1)	0.008(1)	0.009(1)	0.008(1)	0.008(1)
Te	0.010(1)	0.012(1)	0.007(1)	0.009(1)	0.009(1)	0.012(1)
interatomic distances						
Tl−Te (Å)	3.4808(7)	3.5379(4)	3.4697(8)	3.5244(16)	3.5011(10)	3.5658(9)
	3.6548(7)	3.6138(4)	3.6425(9)	3.5918(17)	3.6262(10)	3.5884(9)
Tl−Tl (Å)	3.5388(9)	3.6086(3)	3.5342(7)	3.579(3)	3.4815(13)	3.5539(8)
A−Te (Å)	2.8430(7)	2.8705(7)	2.8428(14)	2.8542(16)	2.7765(9)	2.7992(12)
X−Te (Å)	2.6156(7)	2.7743(7)	2.6177(14)	2.7689(15)	2.6110(9)	2.7702(11)

compounds presented here, has shown promising TE properties at high temperatures.[9] These facts lead us to believe that an advanced TE material may be found among Tl chalcogenides. Our continued investigation into Tl-containing systems led to the discovery of the six isostructural compounds Tl_2AXTe_4 (A = Cd, Hg, Mn, X = Ge, Sn).

In what follows we present the syntheses, crystal structures, calculated electronic structures, and measured TE properties of these new compounds. We also compare the calculated electronic structure of $TlInTe_2$ (a compound with a crystal structure from which the Tl_2AXTe_4 crystal structure can be derived) with that of its isostructural alkali-metal analogue $KInTe_2$.[10]

The experimental details regarding the synthesis and characterization of these compounds as well as the computational details of the DFT calculations can be found in the Supporting Information.

Results and Discussion

Crystal Structure. The results from the single-crystal structure refinements for all six compounds are presented in Table 1. The crystal structure is shown in Figure 1. All compounds are isostructural and crystallize in the noncentrosymmetric, tetragonal space group I-42m. The structure is an ordered superstructure of the TlSe structure type.[11] TlSe (space group $I4/mcm$) consists of 1-D chains of edge-sharing Tl^{3+}-centered tetrahedra, with Se at the vertices, separated by Tl^{1+} ions. The tetrahedrally coordinated Tl^{3+} can be replaced with other trivalent atoms, as in $TlMSe_2$ (M = Al, Ga, In) and $TlMTe_2$ (M=Ga, In).[12] In Tl_2AXTe_4 this tetrahedral site is occupied by divalent and tetravalent atoms in alternation along the chains (Figure 1), and the formal charges can be assigned as $[Tl^{1+}]_2[A^{2+}][X^{4+}][Te^{2-}]_4$.

If the A and X atoms shared the tetrahedral sites instead of being ordered along the chains, this would result in a centrosymmetric structure, isostructural to $TlInTe_2$, with space group $I4/mcm$. Inspection of the systematic absence conditions showed no evidence for a c glide along the a direction, and no evidence of site mixing was seen during the structure refinements. This ensures that the A and X cations are ordered along the chains. The nonzero Flack absolute structure parameters seen for several of these compounds (Table 1) are then attributed to the presence of a racemic mixture in the crystals used for diffraction studies. The refinements for these compounds were carried out using the appropriate twinning law (inversion of all indices).

In all six compounds Tl, A, and X are located at the positions (0 1/2 0), (0 0 1/2), and (0, 0, 0), respectively. Te

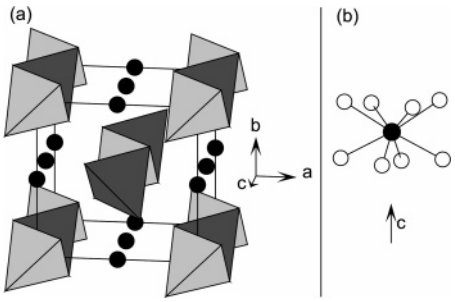

Figure 1. (a) A view of the crystal structure of Tl_2AXTe_4 (A = Cd, Hg, Mn; X = Ge, Sn). The Tl atoms (dark circles) separate chains of edge-sharing A-centered tetrahedra (medium gray) and X-centered tetrahedra (light gray) with Te at the vertices. (b) Distorted square antiprismatic coordination of Tl by Te (open circles).

(8) Kurosaki, K.; Uneda, H.; Muta, H.; Yamanaka, S. *J. Alloys Compd.* **2004**, *376*, 43.
(9) Godzhaev, E. M.; Kerimova, R. A. *Inorg. Mater.* **2004**, *40*, 1153.
(10) Hung, Y.-C.; Hwu, S.-J. *Acta Crystallogr.* **1993**, *C49*, 1588.
(11) Ketalaar, J. A.; t'Hart, W. H.; Moerel, M.; Polder, D. *Z. Kristallogr.***1939**, *A101*, 396.
(12) $TlAlSe_2$ and $TlGaSe_2$: Range, K.-J.; Mahlberg, G.; Obenland, S. *Z. Naturforsch., B* **1977**, *32*, 1354. $TlInSe_2$, $TlGaTe_2$, and $TlInTe_2$: Müller, D.; Eulenberger, G.; Hahn, H. *Z. Anorg. Allg. Chem.* **1973**, *398*, 207.

is at (*x x z*), where *x* and *z* for each compound are given in Table 1. The Tl^{1+} ion is coordinated to eight Te atoms, two from each of four neighboring $[AXTe_4]^{2-}$ chains, in a distorted square antiprismatic environment (Figure 1). This relatively symmetric environment suggests that the Tl^{1+} lone pair is not stereochemically active.

Interatomic distances in each compound are listed in Table 1. The A−Te and X−Te distances are similar to those found in the literature for the corresponding cation oxidation state in tetrahedral coordination: Cd−Te = 2.81 Å in CdTe,[13] Hg−Te = 2.79 Å in HgTe,[14] Mn−Te = 2.75 Å in K_2MnTe_2,[15] Ge−Te = 2.62−2.64 Å in Tl_2GeTe_5,[16] Sn−Te = 2.79 Å in Tl_2SnTe_5.[17] The Tl−Te distances are also consistent with those found in similar known compounds: 3.55−3.71 Å in $Tl_2Cu_2SnTe_4$ and $Tl_2Ag_2SnTe_4$,[5] 3.57 Å in $TlGaTe_2$,[12] 3.60 Å in $TlInTe_2$.[12]

Although we know of no alkali-metal compound which is strictly isostructural to Tl_2AXTe_4, the structure is quite similar to that of $Cs_2MnSnTe_4$.[18] The same $[MnSnTe_4]^{2-}$ chains exist in this compound and are separated by Cs^{1+} ions. However, the arrangement of the chains within the unit cell is different, and the compound is orthorhombic. The structure is also similar to that of $K_2Ag_2SnTe_4$[19] and its Tl analogues $Tl_2Ag_2SnTe_4$ and $Tl_2Cu_2SnTe_4$.[5] In these compounds the divalent A in Tl_2AXTe_4 is replaced by two monovalent ions (Cu or Ag) distributed over four positions surrounding the site occupied by A. There are several known alkali-metal analogues of the parent structure $TlInTe_2$. One example is $KInTe_2$.[10] Below we will compare the calculated electronic structure of these two compounds and see the effect of replacing K with Tl.

Electronic Structure. The electronic structures of these compounds were investigated with density functional theory (DFT) calculations using the full potential linearized augmented plane wave method. First a test calculation was preformed on the compound $TlGaTe_2$. This proved to be in agreement with previous results[20] with the exception of the value of the band gap. Our calculation showed a small positive gap, while Okazaki et al. calculated a small negative gap.[20] Experimentally $TlGaTe_2$ is a semiconductor,[21] in agreement with our calculation. However, it is well known that band gaps determined from DFT calculations can be unreliable and are often underestimated.

We then proceeded to calculate and compare the electronic structures of the isostructural compounds $KInTe_2$[10] and $TlInTe_2$[12] from which the Tl_2AXTe_4 structure can be derived (vide supra). The results are shown in Figure 2. We see that

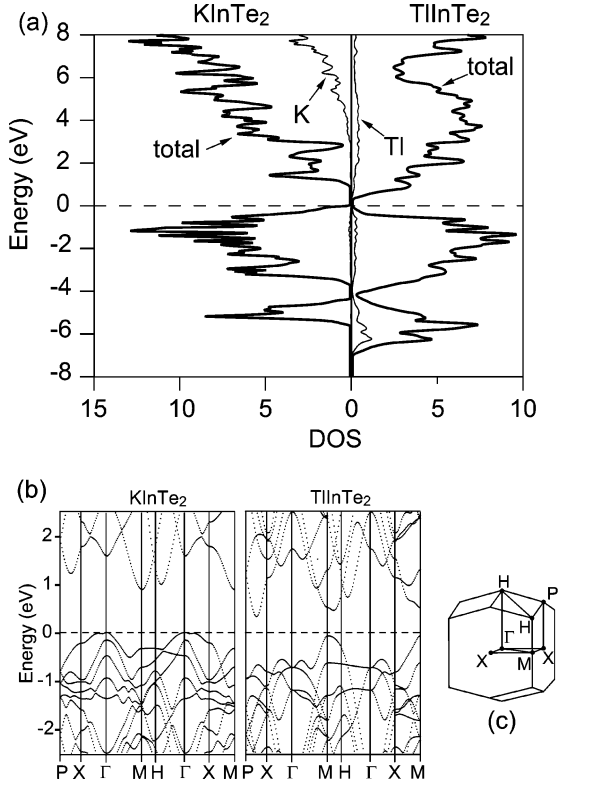

Figure 2. (a) Calculated density of states for $KInTe_2$ and $TlInTe_2$. Also shown are the K and Tl projections. (b) Calculated band structure of $KInTe_2$ and $TlInTe_2$. (c) The first Brillouin zone for the body-centered tetragonal lattice showing the special points as labeled in the band structures. The dashed line in a and b is the Fermi level ($E = 0$ eV).

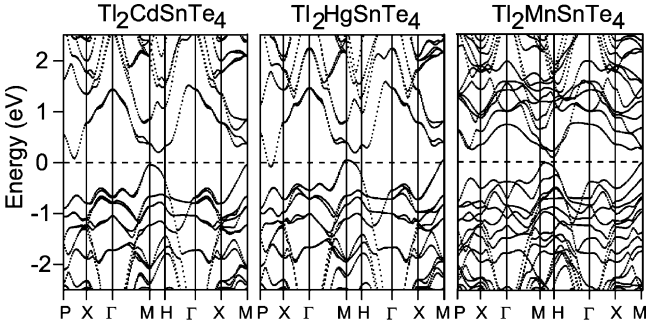

Figure 3. Calculated band structures of $Tl_2CdSnTe_4$, $Tl_2HgSnTe_4$, and $Tl_2MnSnTe_4$. The results for the Ge compounds are similar and included in the Supporting Information. The Fermi level is the dashed line at $E = 0$ eV.

replacing K with Tl decreases the *calculated* band gap. This is consistent with the many experimental examples, which we have previously documented, of the smaller band gaps in Tl compounds compared to their alkali-metal analogues.[5] More importantly, we also see (Figure 3) that the contribution from Tl near the Fermi level, although small, is significantly larger than that of K. This is a direct result of the less electropositive nature of Tl, allowing significant mixing between Tl and Te orbitals near the Fermi level. This means that transport properties should be less anisotropic in a "layered" or "chainlike" Tl compound than in its alkali-metal analogue. This is also reflected in the band structures shown in Figure 2. More dispersion is seen in the bands of $TlInTe_2$ than in the K analogue, especially in the highest valence band.

(13) Rabadanov, M. Kh.; Verin, I. A.; Ivanov, Yu. M.; Simonov, V. I. *Kristallografiya* **2001**, *46*, 703.
(14) Werner, A.; Hochheimer, H. D.; Stroessner, K.; Jayaraman, A. *Phys. Rev. B* **1983**, *28*, 3330.
(15) Bronger, W.; Balk-Hardtdegen, H.; Schmitz, D. *Z. Anorg. Allg. Chem.* **1989**, *574*, 99.
(16) Marsh, R. E. *J. Solid State Chem.* **1990**, *87*, 467.
(17) Agafonov, V.; Legendre, B.; Rodier, N.; Cense, J. M.; Dichi, E.; Kra, G. *Acta Crystallogr.* **1991**, *C47*, 850.
(18) Zimmerman, C.; Dehnen, S. *Z. Anorg. Allg. Chem.* **2003**, *629*, 1553.
(19) Li, J.; Guo, H.-Y.; Proserpio, D. M.; Sironi, A. *J. Solid State Chem.* **1995**, *117*, 247.
(20) Okazaki, K.; Tanaka, K.; Matsuno, J.; Fujimori, A.; Mattheiss, L. F.; Iida, S.; Kerimova, E.; Mamedov, N. *Phys. Rev. B* **2001**, *64*, 045210.
(21) Hanias, M. P.; Anagnostopoulos, A. N. *Phys. Rev. B* **1993**, *47*, 4261.

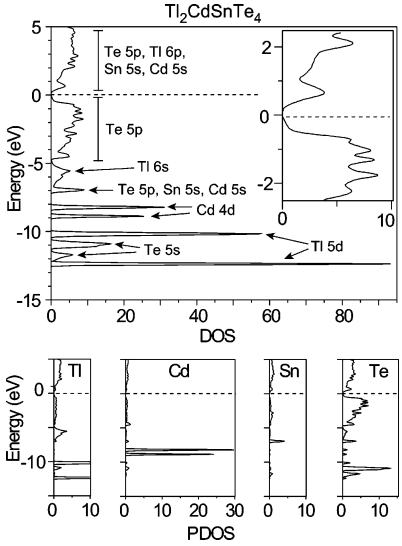

Figure 4. Calculated density of states (DOS) and projected densities of states (PDOS) for $Tl_2CdSnTe_4$. The Fermi level (dotted line) is at $E = 0$ eV. The results for $Tl_2CdGeTe_4$ are similar and included in the Supporting Information.

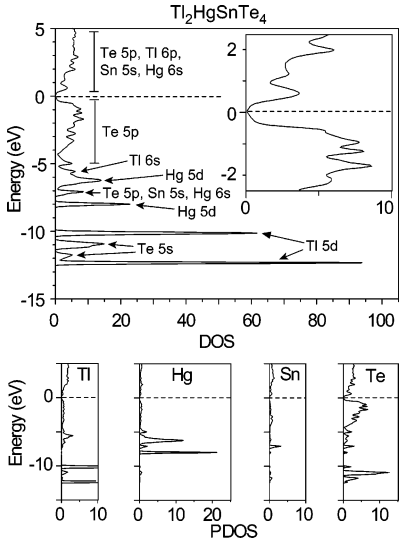

Figure 5. Calculated density of states (DOS) and projected densities of states (PDOS) for $Tl_2HgSnTe_4$. The Fermi level (dotted line) is at $E = 0$. The results for $Tl_2HgGeTe_4$ are similar and included in the Supporting Information.

The calculated band structures of $Tl_2CdSnTe_4$, $Tl_2HgSnTe_4$, and $Tl_2MnSnTe_4$ are shown in Figure 3 and the calculated density of states (DOS) in Figures 4, 5, and 6, respectively. In Figures 4−6 the top panels display the total DOS with a closer view around the Fermi level in the insets. The lower panels show the normalized projected density of states (PDOS). There is little difference between these results for the Sn compounds and those found for the Ge compounds (which we include in the Supporting Information), so only the Sn compounds will be discussed here.

The calculated band structures of $Tl_2CdSnTe_4$ and $Tl_2HgSnTe_4$ are seen to be quite similar with the main difference being the magnitude of the gap. Experimentally, $Tl_2HgSnTe_4$ behaves like a semiconductor (vide infra), though the calculations predict this material to be a semimetal with a small band overlap (Figure 3). This suggests that the gap has been underestimated by the calculation, a common problem with DFT calculations. The same discrepancy was pointed out above for previous calculations on $TlGaTe_2$.[20]

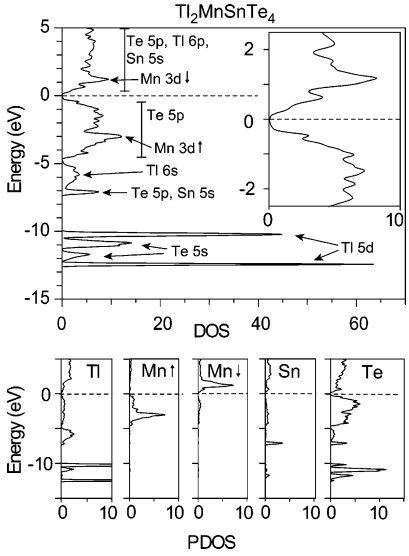

Figure 6. Calculated density of states (DOS) and projected densities of states (PDOS) for $Tl_2MnSnTe_4$. The Fermi level (dotted line) is at $E = 0$. The results for $Tl_2MnGeTe_4$ are similar and included in the Supporting Information.

In the top panels of Figures 4−6 the DOS curves are labeled by the atomic states which make the predominant contributions, as identified by the calculated PDOS. The states near the Fermi level are found to arise primarily from the Te atoms and are identified as the Te 5p bands. The conduction bands contain significant contributions from the cations as well. The filled core levels of Tl (5d and 6s), Cd/Hg (4d/5d), and Te (5s) are visible. The Sn 4d levels are below −15 eV.

Initial, non-spin-polarized calculations predicted $Tl_2MnSnTe_4$ to be metallic with the Fermi level passing through the middle of narrow, half-filled Mn 3d bands. This suggested that these compounds may in fact be Mott insulators.[22] Electrical resistivity and magnetization measurements supported this hypothesis by showing the Mn compounds to be magnetic semiconductors (vide infra). Thus, spin-polarized calculations were performed. These calculations showed (Figures 3 and 6) that the Mn 3d bands are indeed split into spin-up bands which are filled and spin-down bands which are unfilled, confirming that these compounds are Mott insulators.

Thermoelectric Properties: Tl_2AXTe_4 (A = Cd, Hg; X = Ge, Sn). The thermoelectric properties of these four compounds, measured on polycrystalline pellets, are shown in Figure 7. They are seen to be semiconductors with moderately high thermopower at room temperature and very low thermal conductivity. The plateau in the ρ(T) curve for $Tl_2HgGeTe_4$ below about 200 K suggests some unintentional doping may be present in this sample. The Hg compounds have room-temperature resistivities 1−2 orders of magnitude lower than the Cd compounds. The resistivities of all four compounds show activated behavior. Activation energies were estimated from linear fits to $\log(\rho)$ vs $1/T$, assuming ρ

(22) Mott, N. F. *Metal−insulator Transitions*; Taylor and Francis: London, 1974.

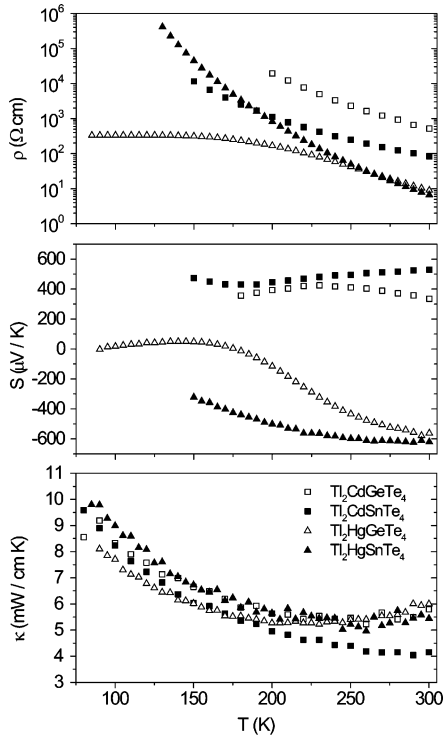

Figure 7. Measured resistivity (ρ), thermopower (S), and thermal conductivity (κ) of Tl_2AXTe_4 (A = Cd, Hg; X = Ge, Sn).

Table 2. Activation Energies from Fitting Resistivity Data, and Band Gaps Determined from Electronic Structures

compound	E_a from ρ data (eV)	calcd gap (eV)
$Tl_2CdGeTe_4$	0.08	0.10
$Tl_2CdSnTe_4$	0.06	0.13
$Tl_2HgGeTe_4$	0.08	−0.18[a]
$Tl_2HgSnTe_4$	0.11	−0.13[a]

[a] Here a negative gap corresponds to a band overlap by that amount.

$\approx \exp(-E_a/k_BT)$. These plots are included in the Supporting Information. The resulting values of E_a, along with band-gap values derived from the band structure calculations, are summarized in Table 2. If the activation is due to excitation across the band gap, the corresponding energy gap equals $2E_a$.

In Figure 7 the Cd compounds are seen to have $S > 0$, while the Hg compounds have $S < 0$. This shows that the dominant charge carriers are holes in the Cd compounds and electrons in the Hg compounds. This may be due to the greater dispersion seen in the conduction band of the Hg compounds (Figure 3).

The temperature dependence of the measured thermal conductivity in Figure 7 is typical for that of crystalline materials. The thermal conductivity of all four materials is very low. For comparison, at room temperature optimized Bi_2Te_3-based alloys have $\kappa \approx 15$ mW/cm K, with a phonon contribution of $\kappa_{ph} \approx 10$ mW/cm K.[2] Due to the relatively high resistivity of these Tl compounds (Figure 8) there is expected to be little electronic contribution to κ. The measured value of κ is essentially equal to κ_{ph}. Other Tl chalcogenides, as noted in the Introduction, have also been found to have low thermal conductivities with values comparable to these materials.

Since these compounds were found to have low κ and high S at room temperature but ρ values too high for TE applications, we tried to prepare doped samples, aiming to decrease ρ while retaining moderately high values of S. The nominally undoped Hg compounds exhibited significantly lower ρ and higher magnitudes of S than the Cd compounds (Figure 8), so we restricted our study to $Tl_2HgGeTe_4$ and $Tl_2HgSnTe_4$. Several dopants were tested: Pb to substitute for Tl (n-type), As (n-type) and Ga (p-type) for Ge, and I for Te (n-type). The target doping density was 10^{19}/cm^3. Since this corresponds to a concentration of only about 0.1%, any second phases which may have formed as a result of the doping were undetectable by X-ray diffraction.

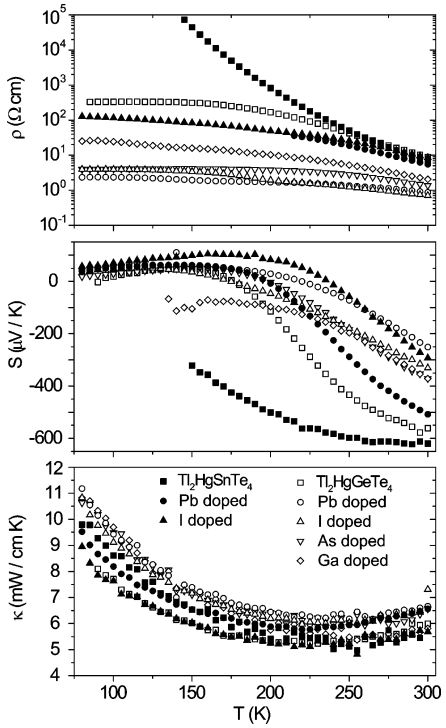

Figure 8. Measured resistivity (ρ), thermopower (S), and thermal conductivity (κ) of doped $Tl_2HgGeTe_4$ and $Tl_2HgSnTe_4$. Data for the undoped compounds are shown for comparison.

The results are shown in Figure 8. The attempted doping produced no significant change in κ. At room temperature the resistivity of $Tl_2HgGeTe_4$ was decreased by about an order of magnitude (to 0.9 Ω cm for I doping) but is seen to be still too high for good TE performance. Although at lower temperatures the resistivity of $Tl_2HgSnTe_4$ was decreased by doping, little difference is seen in the room-temperature values. The thermopower decreased significantly upon doping, by about a factor of 2 in most cases.

The high resistivities of the doped samples suggest that the target carrier concentration was not achieved. This could be due to the formation of compensating defects, which often occurs when doping multinary compounds. Since the doped compounds also had only moderate thermopowers, we did not pursue the doping of these materials further.

Resistivity and Magnetization: Tl_2MnXTe_4 (X = Ge, Sn). The measured magnetic susceptibility per mole of Mn for $Tl_2MnGeTe_4$, measured in an applied field of 2 T and corrected for the diamagnetic response of the sample holder, is shown in Figure 9. The measurements were made on 7.3

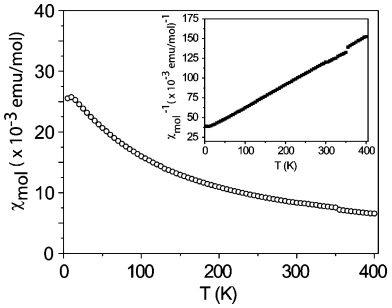

Figure 9. Measured temperature dependence of the molar magnetic susceptibility χ_{mol} and inverse molar magnetic susceptibility (inset) of $Tl_2MnGeTe_4$.

mg of powder ground from single crystals extracted from the polycrystalline reaction product. Powder X-ray diffraction confirmed that the resulting powder was single phase. This compound shows Curie−Weiss-type paramagnetic behavior with evidence of an antiferromagnetic transition visible at the lowest temperatures investigated (Figure 9). We are unsure of the origin of the small discontinuity in the data at 350 K but suspect that it may be due to movement of the sample position within the field. We also note that a field sweep at 300 K showed the sample to be paramagnetic at this temperature, with no sign of saturation up to 5 T.

Fits to the paramagnetic part of the magnetic data below 350 K in Figure 9 were performed using eq 1[23]

$$\chi_{\mathrm{mol}}(T) = \frac{C}{T-\theta}, \mu_{\mathrm{eff}} = \sqrt{\frac{3kC}{N_{\mathrm{A}}}} \qquad (1)$$

Here C is the molar Curie constant, θ is the paramagnetic Curie temperature, k_B is Boltzmann's constant, and N_A is Avogadro's number. Fits suggest a value for θ of −120 K. The negative value of θ shows this compound to be an antiferromagnet. The model gives an effective moment for Mn of $\mu_{eff} = 5.2\ \mu_B$, where μ_B is the Bohr magneton. The effective moment is in only rough agreement with the value of 5.9 μ_B expected for Mn^{2+}.[23] However, eq 1 is expected to be valid only for temperatures well above θ, and we are fitting data only up to $T \approx 3\theta$.[23] This may, in part, account for the disagreement. Although a small difference exists between the expected and measured moments, the data is clearly consistent with localized Mn 3d electrons.

In addition, the resistivities of the Mn compounds, measured on single crystals at room temperature, are high: 4 kΩ cm for $Tl_2MnGeTe_4$ and 5 kΩ cm for $Tl_2MnSnTe_4$. Thus, the measured properties, magnetic and electrical, show the Mn compounds to be Mott insulators, in agreement with the spin-polarized calculations (Figures 3 and 6).

(23) Smart, J. S. *Effective Field Theories of Magnetism*; W. B. Saunders Co.: Philadelphia and London, 1966.

Conclusions

We have presented the synthesis, crystal structure, and electronic structure of the six new quaternary Tl tellurides Tl_2AXTe_4 (A = Cd, Hg, Mn; X = Ge, Sn). These compounds are the first examples of a new variation on the TlSe structure type, with 1-D chains of alternating A- and X-centered tetrahedra which share edges. LAPW band structure calculations predict the Cd compounds to be semiconductors with a small positive gap and the Hg compounds to be semimetals with a small negative gap. Spin-polarized calculations, as well as resistivity and magnetic susceptibility measurements, show the Mn compounds to be Mott insulators due to the narrow half-filled 3d bands of Mn^{2+}.

We have also reported the measured TE properties of the Cd and Hg compounds. These were shown to be small band-gap semiconductors, consistent with the DFT calculations, which are known to underestimate band gaps. At room temperature the compounds also exhibited high thermopower and very low thermal conductivity. However, the electrical resistivities of the samples were too high for TE applications. Our initial investigation into the doping behavior of these compounds produced little improvement in the overall TE performance. The high measured resistivities could be attributed to low carrier concentration due to dopant compensation or grain boundary scattering in the polycrystalline samples.

Acknowledgment. This work was funded by NSF Grant DMR-0011572. We are grateful to Dr. Thomas K. Reynolds for helpful discussions and interactions and Jonathon Petrie for help with the magnetization measurements. We also thank Dr. Emil B. Lobkovsky for assistance in collecting single-crystal X-ray diffraction data and John Hunt for guidance in using the electron microprobe facility in the Cornell Center for Materials Research which is supported through a MRSEC Grant (DMR-0079992). The computational work was supported in part by the Materials Simulation Center, a Penn State Center for Nanoscale Science (MRSEC-NSF) and MRI facility.

Supporting Information Available: Experimental details regarding synthesis, characterization, and crystal structure refinement (including cif files); results of DFT calculations on the Ge-containing compounds; details regarding DFT calculations. This material is available free of charge via the Internet at http://pubs.acs.org.

CM0518067